Czech Technical University in Prague

Faculty of Mechanical Engineering

Department of Process Engineering

Doctoral Thesis Statement

Pool Boiling of Water–Glycerin Mixtures

Viktor Vajc

Doctoral study program: Mechanical Engineering

Branch of study: Design and Process Engineering

Supervisor: *doc. Ing. Radek Šulc, Ph.D.*

Supervisor-specialist: *Ing. Martin Dostál, Ph.D.*

Doctoral thesis statement for the academic degree “Doctor”, abbrev. Ph.D.

Prague *April, 2022*

Title of the thesis: *Pool Boiling of Water–Glycerin Mixtures*

This doctoral thesis was written during full-time doctoral studies at the Department of Process Engineering, Faculty of Mechanical Engineering, CTU in Prague.

Dissertant: Viktor Vajc
Department of Process Engineering
Faculty of Mechanical Engineering, CTU in Prague
Technická street 4, Prague 6, 160 00 Czech Republic

Supervisor: doc. Ing. Radek Šulc, Ph.D.
Department of Process Engineering
Faculty of Mechanical Engineering, CTU in Prague
Technická street 4, Prague 6, 160 00 Czech Republic

Supervisor-specialist: Ing. Martin Dostál, Ph.D.
Department of Process Engineering
Faculty of Mechanical Engineering, CTU in Prague
Technická street 4, Prague 6, 160 00 Czech Republic

Opponents:

The thesis statement was sent out on date:

The defense of the thesis takes place on at : o'clock in conference room no. 17 on the ground floor of the Faculty of Mechanical Engineering, CTU in Prague, Technická street 4, Prague 6, in front of the Thesis Defense Committee for the doctoral study branch *Design and Process Engineering.*

The thesis is available at the Department for Science and Research in the ground floor of the Faculty of Mechanical Engineering, CTU in Prague, Technická street 4, Prague 6.

prof. Ing. Tomáš Jirout, Ph.D.
Head of the Board for doctoral study branch *Design and Process Engineering*
Faculty of Mechanical Engineering, CTU in Prague

Annotation

The doctoral thesis focuses on heat transfer during nucleate boiling of water–glycerin mixtures. In the theoretical part, heat transfer during pool boiling of pure fluids and multicomponent mixtures is outlined and discussed together with the mechanisms and parameters of boiling. The thermophysical properties and boiling behavior of water–glycerin mixtures are also addressed. The second part presents the results of heat transfer measurements during saturated and subcooled nucleate pool boiling of water–glycerin mixtures on copper, nickel-plated, and titanium surfaces. The experiments were performed for wide investigated ranges of the heat flux and concentration of glycerin in the boiling mixture. Heat transfer coefficients (HTCs) were observed to deteriorate with an increasing amount of glycerin in the boiling mixture. A significant impact of the mixture effects on HTC was confirmed for all the mixtures and heating surfaces investigated. For the studied experimental conditions, it was found that subcooled boiling on the nickel-plated surfaces occurred in the developed regime. A method was suggested and verified, which can be used to calculate the subcooled boiling HTC in this regime. During boiling on the thin titanium foil, the bubble departure diameter was found to be weakly dependent on the heat flux and independent of the mixture composition. On the contrary, the nucleation frequency increased with the heat flux and concentration of glycerin in the boiling mixture. Correlations were developed, which does not require knowledge of the thermophysical properties of the boiling mixtures, for a straightforward estimation of the measured HTCs and nucleation parameters.

Keywords

nucleate boiling, pool boiling, saturated boiling, subcooled boiling, water–glycerin mixtures, heat transfer coefficient, mixture effects, experimental measurement, infrared thermometry, correlation

Anotace

Dizertační práce se zabývá přestupem tepla při bublinovém varu binárních směsí voda–glycerin. Teoretická část práce je zaměřena na přestup tepla při objemovém varu čistých kapalin a vícesložkových směsí spolu s mechanismy a nukleačními parametry varu. Jsou zde také diskutovány termofyzikální vlastnosti a chování směsí voda–glycerin při varu. Druhá část prezentuje výsledky experimentálního měření přestupu tepla při nasyceném a podchlazeném bublinovém varu v objemu pro směsi voda–glycerin na měděných, niklovaných a titanových výhřevných površích. Experimenty byly provedeny pro široký rozsah tepelných toků a koncentrací glycerinu ve vroucí směsi. Bylo zjištěno, že s rostoucí koncentrací glycerinu dochází k poklesu součinitele přestupu tepla. Významný vliv tzv. směsných efektů na var byl potvrzen pro všechny zkoumané směsi a výhřevné povrchy. Dále bylo zjištěno, že podchlazený var na poniklovaných površích probíhá za zkoumaných experimentálních podmínek v podchlazeném vyvinutém režimu. Byla navržena a ověřena metoda výpočtu součinitele přestupu tepla v tomto režimu. Při varu na titanové fólii bylo zjištěno, že průměry bublin jsou jen slabě závislé na tepelném toku a nezávislé na složení vroucí směsi. Naopak nukleační frekvence se zvyšovaly jak s tepelným tokem, tak s koncentrací glycerinu ve směsi. Byly navrženy snadno použitelné korelace pro stanovení naměřených součinitelů přestupu tepla a pro hodnoty zkoumaných nukleačních parametrů, které nevyžadují znalost termofyzikálních vlastností vroucích směsí.

Klíčová slova

bublinový var, objemový var, nasycený var, podchlazený var, směs voda–glycerin, součinitel přestupu tepla, směsný efekt, experimentální měření, infračervená termometrie, korelace

1. Introduction

1.1 Heat Transfer during Saturated and Subcooled Boiling

Boiling is a process characterized by intense heat transfer at a relatively low driving temperature difference, which is utilized in various industrial applications. The nucleate boiling regime is characterized by the highest heat transfer coefficients (HTCs) compared with other regimes of pool boiling. Knowledge of HTC during boiling enables cost-saving design and efficient operation of industrial apparatuses.

The HTC during saturated boiling might be defined as

$$\alpha = \frac{q}{T_\mathrm{s} - T_\mathrm{sat}} \,, \tag{1}$$

where q denotes the heat flux, T_s is the temperature of the heating surface, and T_sat is the saturation temperature corresponding to the pressure above the free surface of the boiling liquid. The denominator of Eq. (1) is called the *superheat* of the heating surface

$$\Delta T_\mathrm{sat} = T_\mathrm{s} - T_\mathrm{sat} \,. \tag{2}$$

During subcooled boiling, the temperature of the boiling liquid T_L is lower than T_sat. The *subcooling* of the boiling liquid is defined to be the difference between both temperatures

$$\Delta T_\mathrm{sub} = T_\mathrm{sat} - T_\mathrm{L} \,. \tag{3}$$

It is useful to define the *total* HTC during subcooled boiling

$$\alpha_\mathrm{tot} = \frac{q}{T_\mathrm{s} - T_\mathrm{L}} \tag{4}$$

and the *boiling* HTC during subcooled boiling

$$\alpha_\mathrm{b} = \frac{q}{T_\mathrm{s} - T_\mathrm{sat}} \,. \tag{5}$$

The relation between the *total*- and the *boiling* HTC is then

$$\frac{1}{\alpha_\mathrm{tot}} = \frac{1}{\alpha_\mathrm{b}} + \frac{\Delta T_\mathrm{sub}}{q} \,. \tag{6}$$

The fraction $(q/\Delta T_\mathrm{sub})$ in Eq. (6) represents the heat transfer resistance due to convection in the liquid bulk and condensation of bubbles in the subcooled liquid. Although a higher subcooling is able to increase the *boiling* HTC, it usually lowers the *total* HTC. Saturated boiling might be considered to be superior to subcooled boiling due to higher values of the *total* HTC α_tot [1].

1.2 Correlations for Heat Transfer during Saturated Boiling of Pure Fluids

It is possible to correlate the HTC during saturated pool boiling using the simple empirical power function

$$\alpha = C\, q^n \,, \tag{7}$$

where the coefficient C depends on the combination of the boiling liquid and heating surface. The exponent n is typically in the range $0.6 < n < 0.8$ [2]. However, for engineering calculations, some more complex heat transfer correlations are usually applied which typically assume a dependency of HTC on the thermophysical properties of the boiling fluid, the thermophysical properties of the heating surface, or on other conditions (the roughness of the heating surface, pressure, contact angle, and others). The various parameters of correlations are often combined into dimensionless complexes, such as the Reynolds number or the Nusselt number. A plethora of heat transfer correlations have been published in the literature dealing with pool boiling. Two representatives might be the universal correlation of Stephan and Abdelsalam [3]

$$\frac{\alpha\, D_\mathrm{b}}{\lambda_\mathrm{L}} = 0.23 \left(\frac{q\, D_\mathrm{b}}{\lambda_\mathrm{L}\, T_\mathrm{sat}}\right)^{0.674} \left(\frac{\varrho_\mathrm{G}}{\varrho_\mathrm{L}}\right)^{0.297} \left(\frac{\Delta h_\mathrm{LG}\, D_\mathrm{b}^2}{a_\mathrm{L}^2}\right)^{0.371} \left(\frac{\varrho_\mathrm{L} - \varrho_\mathrm{G}}{\varrho_\mathrm{L}}\right)^{-1.73} \left(\frac{a_\mathrm{L}^2\, \varrho_\mathrm{L}}{\sigma\, D_\mathrm{b}}\right)^{0.35} \tag{8}$$

or the correlation of Yagov[4]

$$q = 3.43 \times 10^{-4}\, \frac{\lambda_\mathrm{L}^2\, \Delta T^3}{\nu_\mathrm{L}\, \sigma\, T_\mathrm{sat}} \left(1 + \frac{\Delta h_\mathrm{LG}\, \Delta T\, M_\mathrm{m}}{2\, R_\mathrm{m}\, T_\mathrm{sat}^2}\right)\left(1 + \sqrt{1 + 800\, C_\mathrm{b}} + 400\, C_\mathrm{b}\right) , \tag{9}$$

where the saturation temperature T_sat is in kelvins and the dimensionless boiling parameter C_b is defined as

$$C_\mathrm{b} = \frac{\Delta h_\mathrm{LG}\, (\varrho_\mathrm{G}\, \nu_\mathrm{L})^{3/2}}{\sigma\, (\lambda_\mathrm{L}\, T_\mathrm{sat})^{1/2}} \,. \tag{10}$$

1.3 Deterioration of HTC during Pool Boiling of Mixtures

Boiling of mixtures is typical for the separation of individual components during distillation. Besides that, boiling of suitable mixtures is often utilized in various industrial apparatuses, because it might bring some benefits over boiling of pure single-component fluids, such as improved thermodynamic efficiency [5], improved cooling capacity [6], or enhancement of thermophysical properties of the mixture [7]. On the other hand, boiling of mixtures has two major disadvantages with respect to boiling of pure fluids: (1) the deterioration of HTC during mixture boiling and (2) the fact that the boiling performance is way more difficult to predict for mixtures compared with boiling of pure fluids.

The HTC during boiling of mixtures might be defined by the equation

$$\alpha = \frac{q}{T_\mathrm{s} - T_\mathrm{b}} \,, \tag{11}$$

which is similar to Eq. (1), but the saturated temperature T_sat was substituted by the *bubble-point* temperature T_b which is now a function of the liquid composition. The liquid composition is typically expressed using molar fractions x_i or mass fractions ω_i, where i is the ordinal number of the mixture components ordered in descending order according to their volatility ($i = 1$ corresponds to the most volatile, $i = 2$ to the second most volatile, etc.).

The HTC during boiling of mixtures can be related to the so-called *ideal* HTC using the equation

$$\alpha = \frac{\alpha_\mathrm{id}}{1 + F} \,, \tag{12}$$

where the *ideal* HTC α_id can be interpolated between the HTCs of pure components or estimated from a pure fluid correlation using the thermophysical properties of the boiling mixture. The correction factor $F \geq 0$ accounts for the impact of the so-called *mixture effects* on boiling. The correction factor F is the most often correlated parameter related to heat transfer during boiling of mixtures.

1.4 Correlations for HTC during Boiling of Binary Mixtures

Boiling of binary mixtures is the main target of researchers, since boiling of mixtures with three or more components is too complex and the published data are inconsistent, limited, and difficult to interpret [8]. Although generalized correlations for the mixtures with three or more components can be found in the literature, the most published and verified correlations are applicable only for binary mixtures. A typical heat transfer correlation for binary mixtures contains one or more of the following parameters:

- Some quantities related to mass transfer, such as the binary diffusion coefficient D_{12} or the mass transfer coefficient in the liquid phase β_L.
- The equilibrium molar fraction difference $|y_i - x_i|$, where y_i is the molar fraction of the vapor phase in equilibrium with the liquid phase of the molar fraction x_i.
- The boiling range $\Delta T_\mathrm{db} = T_\mathrm{d} - T_\mathrm{b}$ which is the difference between the *dew-point* and the *bubble-point* temperature.
- Various thermophysical properties of the boiling fluid (density, latent heat of vaporization, surface tension, etc.).
- Other parameters, such as the heat flux q or the pressure p.
- Empirical coefficients which might be tuned for a particular boiling mixture.

As in the case of pure fluids, a plethora of correlations can be found in the literature which were developed for boiling of binary mixtures. A representative

might be the influential correlation of Schlünder [9]

$$F = \frac{\alpha_{\mathrm{id}}}{q} \left(T_{\mathrm{sat},2} - T_{\mathrm{sat},1}\right) \left(y_1 - x_1\right) \left[1 - \exp\left(\frac{-C_0\, q}{\varrho_{\mathrm{L}}\, \Delta h_{\mathrm{LG}}\, \beta_{\mathrm{L}}}\right)\right], \tag{13}$$

where $(T_{\mathrm{sat},2} - T_{\mathrm{sat},1})$ is the difference between the temperatures of both pure components and C_0 is an empirical coefficient (called the *scaling factor*). Schlünder [9] recommended to use the values $C_0 = 1$ and $\beta_{\mathrm{L}} = 2 \times 10^{-4}\ \mathrm{m\,s^{-1}}$. Thome and Shakir [10] suggested to use $C_0 = 1$ and to find the optimal mass transfer coefficient in the range $1 \times 10^{-4} \leq \beta_{\mathrm{L}} \leq 5 \times 10^{-4}\ \mathrm{m\,s^{-1}}$.

Another representative is the correlation published by Inoue and Monde [11]

$$F = \frac{\alpha_{\mathrm{id}}}{q} \left\{ a\, C\, \Delta T_{\mathrm{db}} + b \left(T_{\mathrm{sat},2} - T_{\mathrm{sat},1}\right) \left(y_1 - x_1\right) \left[1 - \exp\left(\frac{-C_0\, q}{\varrho_{\mathrm{L}}\, \Delta h_{\mathrm{LG}}\, \beta_{\mathrm{L}}}\right)\right] \right\}, \tag{14}$$

which is a linear combination of the Schlünder correlation (13) and of the correlation proposed by Inoue et al. [12]. Correlation (14) was developed to include the effects of $|y_i - x_i|$ as well as ΔT_{db} on the deterioration of HTC. Inoue and Monde [11] recommend to use the values of coefficients $a = 0.15$, $b = 0.25$, $C_0 = 1$, and $\beta_{\mathrm{L}} = 2 \times 10^{-4}\ \mathrm{m\,s^{-1}}$.

2. Boiling of Water–Glycerin Mixtures

2.1 Production and Utilization of Glycerin

At present, there is a surplus of glycerin on the global market, which is mainly caused by the biodiesel production. Approximately 90 % of the worldwide amount of glycerin stems from the transesterification of triglycerides to biodiesel [13]. OECD estimates that more than $5 \times 10^6\ \mathrm{m^3}$ of glycerin was produced in 2020 [14].

Boiling of glycerin mixtures typically takes place inside of distillation columns after they were used in extractive distillation or absorption. Other ways of glycerin utilization are expected to be developed in the future, which will reduce the cost of the produced biodiesel. Although there is growing interest and intensive research aimed towards glycerin utilization, the thermophysical, chemical, and transport properties of glycerin and its mixtures need to be thoroughly studied to find the most suitable and efficient methods.

2.2 Boiling Behavior of Water–Glycerin Mixtures

Glycerin is an environmentally friendly trivalent alcohol which is a colorless, odorless, sweet-tasting, nontoxic, hygroscopic viscous liquid with a high boiling point [15]. Glycerin is fully miscible with water [13]. Water–glycerin mixtures exhibit Newtonian behavior and are characterized by a significant difference between the viscosities of both pure components [15].

The vapor–liquid equilibrium calculated with the non-random two-liquid model presented by Mokbel et al. [16] is shown in Fig. 1. The vapor–liquid

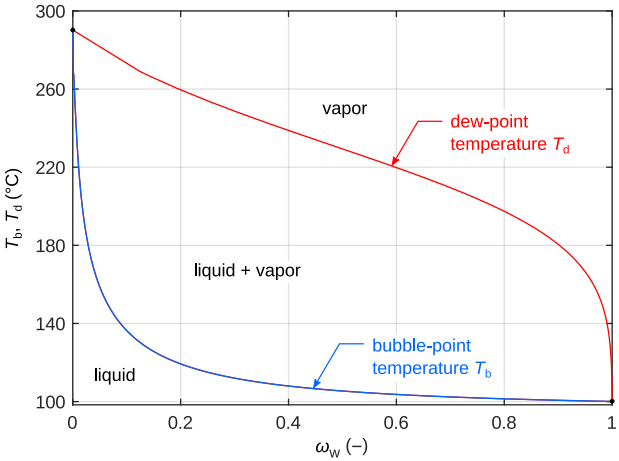

Figure 1: The vapor–liquid equilibriums of water–glycerin mixtures at atmospheric pressure calculated with the model of Mokbel et al. [16].

equilibrium of water–glycerin mixtures is characterized by the following facts:

- The vapor, which is in equilibrium with the liquid in the water mass fraction range $\omega_w > 0.10$, is composed almost solely of water (the molar fraction of the vapor $y_w > 0.999$).
- The *bubble-point* temperature T_b is weakly dependent on ω_w for mixtures with a high water content ($\omega_w \gtrsim 0.20$).
- The mixtures of water and glycerin have a high boiling range $\Delta T_{db} = T_d - T_b$ for almost all liquid compositions ($\Delta T_{db} > 50$ °C in the range of water mass fractions $0.01 < \omega_w < 0.98$).
- The mixtures of water and glycerin are characterized by a significant difference of the saturation temperatures of both pure components of about 190 °C at atmospheric pressure.

Boiling of water–glycerin mixtures is significantly affected by the facts listed above. For instance, it was reported [17] that bubble departure diameters should be independent of the liquid composition in the range $\omega_w > 0.30$ which is a consequence of the fact that the *bubble-point* temperature T_b and the equilibrium molar fraction of the vapor phase y_i both remain more or less constant and independent of variations of ω_w.

2.3 Literature Dealing with Boiling of Water–Glycerin Mixtures

According to the works focused on pool boiling of water–glycerin mixtures, which are listed in Tab. 1, HTC deteriorates with increasing concentration of glycerin in the boiling mixture, which is explained by the authors to be the consequence of the various *mixture effects* which are present during boiling.

Table 1: The reported experimental measurements of the HTC during pool boiling of water–glycerin mixtures.

Authors	Surface	Material	Pressure	ω_w (−)	q (kW m^{-2})
Sternling and Tichacek [18]	tube	stainless steel	atmospheric	0.00 to 0.75	25 to 495
Sarafraz et al. [19]	tube	stainless steel	atmospheric[1]	0.95 to 0.99	5 to 92
Alavi Fazel et al. [20]	tube	stainless steel	atmospheric	0.65 to 1.00	up to 92
Kuo [21][2]	tube	*Inconel 600*	atmospheric	0.03 to 0.20	up to 1 350
McNeil et al. [22]	bundle	brass	20 kPa[3]	0.38[4]	10 to 65

[1] The boiling pressure is not explicitly stated. Authors report just the degassing pressure from 10 to 15 kPa.
[2] Although Kuo [21] discuss the film boiling of water–glycerin mixtures to decompose glycerin into syngas, he published results for four runs of nucleate boiling.
[3] The reported pressure of 5 kPa above the liquid level and the tube bundle submerged approximately 1.6 m deep into water give a local pressure of about 20 kPa.
[4] The concentration of the boiling mixture was estimated from viscosity measurements.

Alavi Fazel et al. [20] and Yang et al. [23] reported a minor HTC enhancement of about 20 % during pool and flow boiling of mixtures with a low amount of glycerin ($\omega_w \gtrsim 95$ %) at heat fluxes lower than 85 kW m^{-2}. Furthermore, Alavi Fazel et al. [20] suggested that for mixtures with $\omega_w > 0.65$, HTC corresponds to the *ideal* HTC and that the *mixture effects* might be neglected in the heat flux range $q < 70$ kW m^{-2}.

Alavi Fazel et al. [20] were able to successfully correlate their boiling data with the combination of the Stephan and Abdelsalam correlation and the correlation of Schlünder, see Eq. (8) and (13), respectively. Sarafraz and Peyghambarzadeh [19] noted that the authors of heat transfer correlations typically do not specify how to obtain the thermophysical properties of the boiling fluid and that calculated HTCs strongly depend on the employed values of thermophysical properties.

The mixtures of water and glycerin are stable in wide ranges of water mass fractions and temperatures. However, for the mixtures in the range $\omega_w < 0.06$, glycerin is prone to thermal decomposition due to the increase of the *bubble-point* temperature [17].

3. The Objectives of the Thesis

The following research goals related to nucleate pool boiling of water–glycerin mixtures were set based on the review of the available literature:

- Measure HTCs for flat (planar) heating surfaces. In the literature, all reported experiments were done with tubes, see Tab. 1.
- Investigate the boiling performance on copper, nickel, and titanium surfaces. Experiments performed for the three different surface materials might reveal some general trends valid for water–glycerin mixtures rather than for a specific liquid–surface combination.
- Measure HTCs for mixtures with a lower glycerin content boiling at medium and higher heat fluxes. Tab. 1 shows that in the range $0.75 \leq \omega_w \leq 1.00$, the mixtures were investigated only at a relatively low heat flux $q < 92\ \mathrm{kW\,m^{-2}}$.
- Study the impact of the *mixture effects* on the HTC during boiling of water–glycerin mixtures.
- Analyze the possible HTC enhancement reported in the literature for mixtures with a low concentration of glycerin boiling on stainless steel surfaces. The enhancement was not verified for planar surfaces or different materials of the heating surface.
- Evaluate bubble departure diameters, nucleation frequencies, and bubble growth rates, based on the analysis of the infrared (IR) footage of bubble nucleation, which has never been done before. Based on the measured values, suggest the governing heat transfer mechanisms during boiling of water–glycerin mixtures.
- Measure HTCs during subcooled boiling of water–glycerin mixtures and compare them with the corresponding saturated HTCs. The heat transfer performance during subcooled boiling of mixtures is largely unexplored.
- Develop simple suitable correlations which could be employed to quickly estimate HTC and do not require knowledge of the thermophysical properties of the boiling fluid.
- Investigate the stability and performance of the tested surfaces in time. The stability and repeatability of the boiling performance is rarely addressed and overlooked in the literature.

4. Experiments with Thick Copper Sample

Although copper is the most often studied material of the heating surface in the literature dealing with boiling, experiments with boiling of water–glycerin mixtures on copper surfaces have not yet been performed. In this section, the results of experimental measurements obtained during saturated nucleate pool boiling of water–glycerin mixtures on a smooth copper surface are presented and discussed. Boiling was investigated at atmospheric pressure, at heat fluxes from 25 up to 270 kW m^{-2} and for water mass fractions from 1.00 (pure water) down to 0.40. The obtained results presented and discussed in this section were previously published in our article [24].

4.1 Experimental Apparatus

The experiments were performed using the experimental apparatus shown in Fig. 2. The apparatus is opened to the surroundings. During boiling of the studied mixtures, water was continuously pumped into the apparatus with a dosing pump to maintain a constant composition and a constant level of the boiling mixture during measurements. The main part of the apparatus is the cubic copper block heated by five heating cartridges whose square top face with dimensions of 48 × 48 mm and roughness R_a of about 0.4 µm, serves as the heating surface

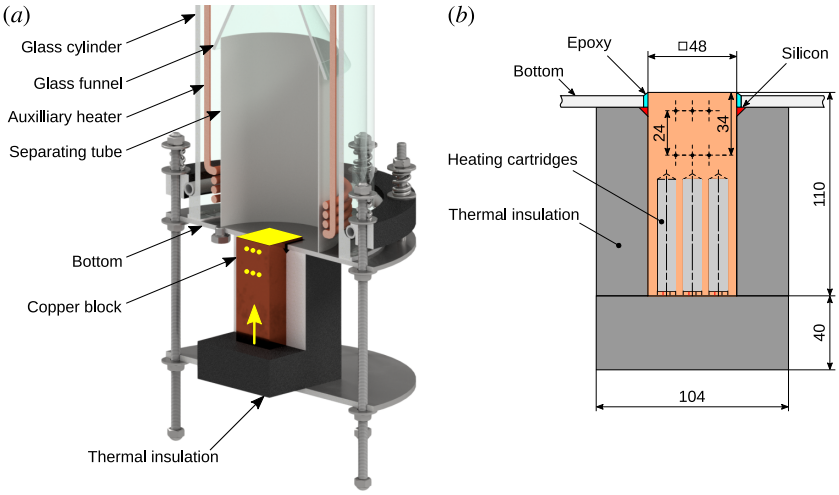

Figure 2: The experimental apparatus designed at CTU in Prague: (*a*) The assembled apparatus. Yellow color marks the heating surface, six thermocouple holes, and orientation of the heating cartridges inside the copper block. Adopted from Vajc et al. [24]. (*b*) Cross-section view with the dimensions of the copper block.

on which boiling takes place. The temperature field inside the block is measured with six sheathed K-type thermocouples (TCs) with a diameter of 1 mm placed into two rows and three columns, which enables one to take the local distribution of the HTCs above the heating surface into account. The temperature of the boiling liquid was measured with two K-type TC probes submerged in the liquid above the heating surface.

4.2 Static and Dynamic Method of Measurement

Besides the commonly employed static measurement method, during which each HTC is measured in the steady-state of boiling, a new dynamic method was proposed and tested. Može et al. [25,26] showed that a continuous increase of heat flux during measurements does not impact the measured HTCs when the increase is sufficiently slow. This was also verified by numerical simulations published in the supplementary information of one of our studies [27].

At CTU, we have also developed a dynamic method for measurement of the HTC during boiling of mixtures, which enables to measure the HTC as a function of concentration of the boiling mixture in a single experimental run. This speeds-up measurements compared with the ordinary steady-state method [24]. When the method is applied, water vapors are allowed to escape the opened apparatus during each experimental run. This leads to a continuous change of the actual concentration of the boiling mixture and to a corresponding variation of the measured HTC. The investigated mixture is boiled until the liquid level drops close to the heating section of the auxiliary heater. The experiments are then stopped to prevent air coming into contact with the heater.

4.3 Measurement Uncertainties

The theory of propagation of the uncertainty was used to estimate the uncertainty of HTC $u(\alpha)$ for performed measurements. The calculated uncertainties $u(\alpha)$ are given in Tab. 2 for low, medium, and high investigated heat flux, together with experimental conditions. The resulting values $u(\alpha)$ indicate that to lower the uncertainty below 20 %, the measurements should be performed at heat fluxes higher than approximately 25 kW m^{-2}.

Table 2: The HTC uncertainty $u(\alpha)$ and data measured during boiling of pure water used for its estimation.

Point	$\alpha \pm u(\alpha)$ (kW m^{-2} K^{-1})	q (kW m^{-2})	T_s (°C)	T_b (°C)	p (kPa)
1	2.45 ± 0.57	18.5	105.8	98.2	99.72
2	4.39 ± 0.57	40.0	107.6	98.5	100.24
3	17.56 ± 1.48	191.4	109.6	98.7	100.24

4.4 Results and Discussion of Steady-State Measurements

Measured Data and Suitable HTC Correlations

Fig. 3 shows the HTCs measured during saturated pool boiling of water–glycerin mixtures at atmospheric pressure for water mass fractions form 1.00 (pure water) down to 0.40, values of HTCs predicted for individual concentrations with the combination of the pure-fluid correlation of Stephan and Abdelsalam (8) and the mixture correlation of Schlünder (13), and the experimental data measured by Sternling and Tichacek [18] and by Sarafraz and Peyghambarzadeh [19].

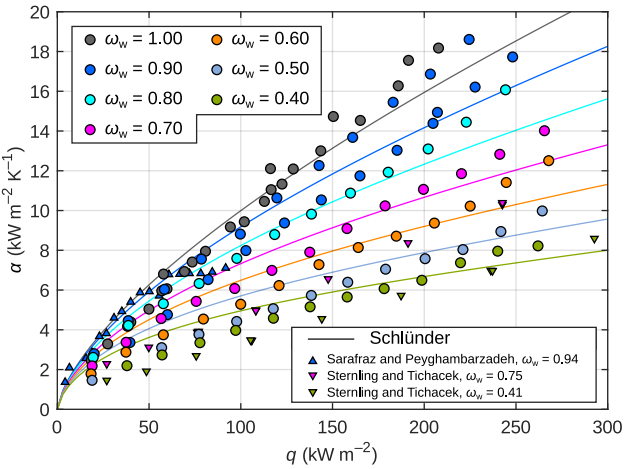

Figure 3: The measured data compared with the data of Sarafraz and Peyghambarzadeh [19], with the data of Sternling and Tichacek [18], and with the Schlünder correlation [9] evaluated using the coefficients $C_0 = 1$ and $\beta_L = 2 \times 10^{-4}$ m s^{-1}. α_{id} was calculated with the correlation of Stephan and Abdelsalam [3]. Published in [24].

The correlated values correspond quite well to the measured HTCs. A standard error of the estimate (SEE) of 1.0 kW m^{-2} K^{-1} and a mean relative error (MRE) of about 14 % were calculated for the Schlünder correlation evaluated with the values of empirical parameters $C_0 = 1$ and $\beta_L = 2 \times 10^{-4}$ m s^{-1} recommended by Schlünder. The optimization of the empirical coefficient did result only in a negligible improvement of both errors.

Own Empirical Correlation for HTC

An empirical correlation was developed for the investigated water–glycerin mixtures, which does not require knowledge of the thermophysical properties of the boiling mixture and offers a fast and straightforward calculation of HTC.

The correlation

$$\alpha = 0.59\, q^{0.714+0.130\omega_w} \tag{15}$$

can be used for water–glycerin mixtures boiling on copper surfaces in the range of investigated heat fluxes $25 \le q \le 270$ kW m^{-2} and water mass fractions $0.40 \le \omega_w \le 1.00$. The correspondence between the correlation and the measurements is plotted in Fig. 4 which shows that almost all data points do not deviate by more than ±20 % from the predictions of the correlation. To use correlation (15), the heat flux q needs to be in (W m^{-2}), the water mass fraction ω_w is dimensionless and the resulting α is in (W m^{-2} K^{-1}). Errors SEE of 0.5 kW m^{-2} K^{-1} and MRE below 6 % were calculated between the measured and correlated HTCs.

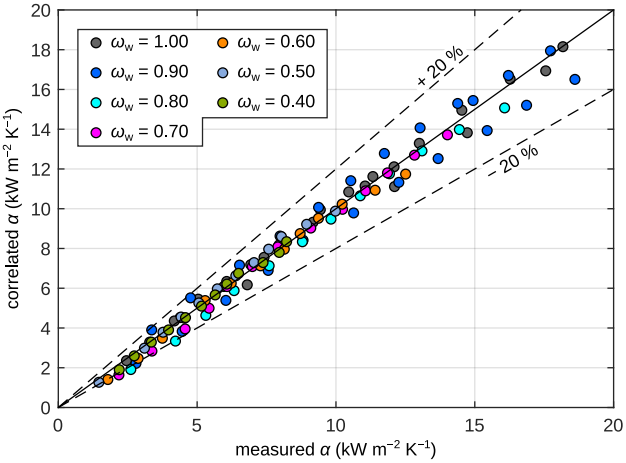

Figure 4: The correspondence between the measured HTCs and empirical correlation (15).

4.5 Results and Discussion of Dynamic Measurements

The dynamic method of measurement was speculatively tested on the water–glycerin mixture with an initial water mass fraction $\omega_w = 0.70$. The mixture was boiled down to $\omega_w = 0.35$. Fig. 5 shows the dependency of HTC on the composition of the boiling mixture and comparison with the steady-state measurements, which are represented by empirical correlation (15). The experimental data correspond quite well to correlation (15) for ω_w from 0.35 to 0.45. For a higher ω_w, the results of the dynamic method are slightly lower relative to the steady-state measurements. Nevertheless, the difference remains acceptable for all investigated concentrations (the maximum deviation between

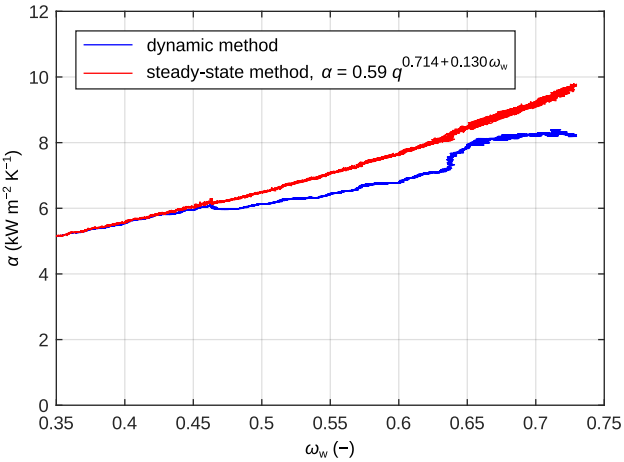

Figure 5: The effect of the actual composition of the boiling liquid on the HTC obtained with the dynamic method of measurement and comparison with correlation (15) which represents the steady-state measurements. Published in [24].

both methods is of about 15 %). The difference between both methods is caused by the flat dependence of the *bubble-point* temperature on the mixture composition, see Fig. 1, which makes the estimation of the actual composition of the mixture difficult. To overcome this, it is either necessary to perform periodic sampling of the boiling liquid or to use more accurate models of the vapor–liquid equilibriums, which need to be based on precise measurements of the temperature of the liquid bulk.

5. Experiments with Thick Nickel-Plated Samples

Chemically nickel-plated copper surfaces were prepared to create a stable heating surface and to eliminate the reported instability and reactivity of copper surfaces [28,29]. Saturated experiments were performed in the heat flux range from 50 to 650 kW m^{-2} for the mixtures with ω_w from 1.00 down to 0.60, followed by subcooled experiments conducted at heat flux levels of approximately 250, 450, and 650 kW m^{-2} at subcooling from 30 down to 0 K. The obtained results presented and discussed in this section were previously published in our article [30].

5.1 Experimental Apparatus

The experiments were performed using the experimental apparatus built by the research team at the Laboratory for Thermal Technology, University of Ljubljana, shown in Fig. 6. The tested sample is heated by three horizontal cartridge heaters. Five identically manufactured cylindrical nickel-plated copper samples (named Sample 1 to Sample 5) were investigated. The flat top nickel-plated face of each tested sample served as the heating surface on which boiling took place. Three vertically aligned unsheathed TCs are used to monitor the temperatures inside

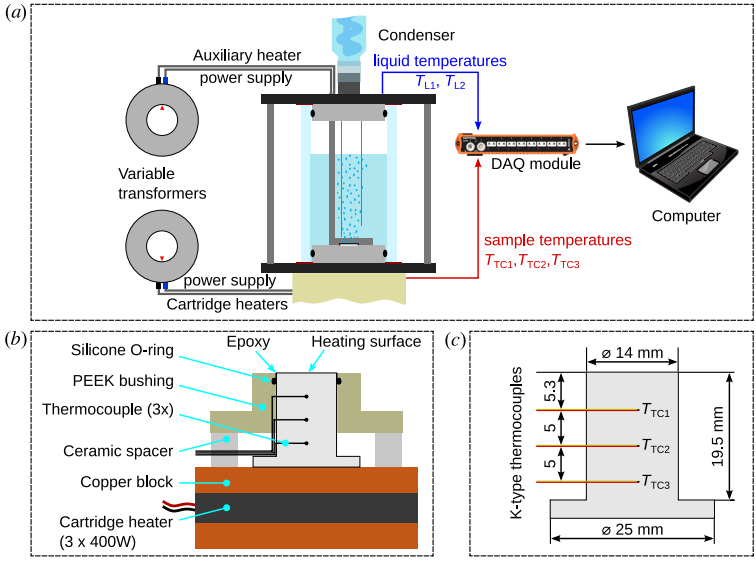

Figure 6: The experimental apparatus for thick samples built by the research team at the Laboratory for Thermal Technology: (*a*) the boiling chamber and equipment, (*b*) the heating assembly, (*c*) the dimensions of the sample and positions of TCs.

the tested sample. The liquid temperature is measured with two sheathed TCs submerged at different depths. An auxiliary immersion heater is used to preheat and degas the boiling liquid before the start of measurements, to maintain the saturation temperature during saturated runs, and to gradually decrease the subcooling of the boiling liquid during subcooled runs. A glass water-cooled condenser is attached to the top flange of the boiling chamber.

5.2 Measurement Uncertainties

The methodology presented by Može et al. [31] was used for calculation of measurement uncertainties. The following uncertainties were evaluated experimentally: 0.16 mm for the distance between neighboring TCs, 0.18 mm for the distance between the uppermost TC and the heating surface, 0.19 K at 100 °C and 0.30 K at 250 °C for temperature measurements. A relative uncertainty of 1.5 % was estimated for the thermal conductivity of the tested blocks. This estimation is based on the accuracy of the performed laser-flash measurements of the thermal diffusivity. The calculated values of the relative uncertainties of HTC $u_\mathrm{r}(\alpha)$, heat flux $u_\mathrm{r}(q)$, and superheat $u_\mathrm{r}(\Delta T_\mathrm{sat})$ are listed in Tab. 3 for a low, medium, and high investigated heat flux.

Table 3: The relative uncertainties of HTC $u_\mathrm{r}(\alpha)$, heat flux $u_\mathrm{r}(q)$, and superheat $u_\mathrm{r}(\Delta T_\mathrm{sat})$ calculated for a low, medium, and high heat flux level. Published in [30].

q (kW m^{-2})	$u_\mathrm{r}(\alpha)$ (%)	$u_\mathrm{r}(q)$ (%)	$u_\mathrm{r}(\Delta T_\mathrm{sat})$ (%)
50	22.3	20.2	2.7
300	5.6	4.1	1.9
650	4.3	2.7	2.0

5.3 Results and Discussion for Saturated Runs

Measured Data and Suitable HTC Correlations

Fig. 7 shows the data points measured during saturated boiling for all the heat fluxes and concentrations investigated. The presented set of data points was obtained by averaging the measured HTCs across all investigated samples. HTC exhibits a deterioration with decreasing ω_w. For all investigated samples, the drop of HTC was more pronounced for higher ω_w and no HTC enhancement was reached for any heat flux and concentration investigated. The observed trends generally agree with the measurements performed on the copper surface presented in Section 4.

Fig. 7 also includes the experimental data published by Sternling and Tichacek [18] and by Vajc et al. [24], which were discussed in Sec. 4. Lower

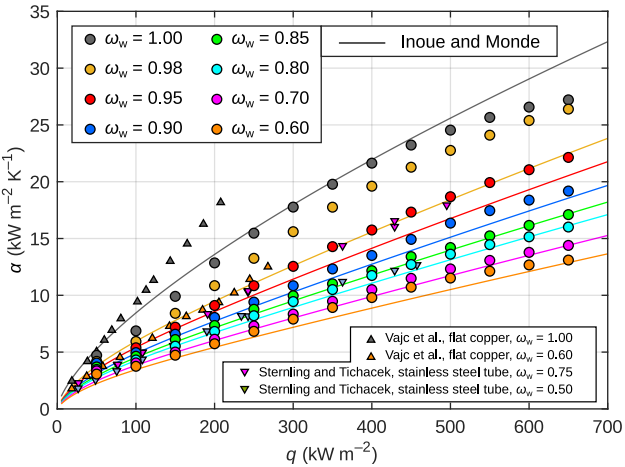

Figure 7: The averaged data set and the predictions of the combination of the mixture correlation of Inoue and Monde [11] and the pure-fluid correlation of Yagov [4]. The empirical coefficients $a = 0.15$ and $b = 0.25$ were employed. Data published by Vajc et al. [24] and Sternling and Tichacek [18] are also shown. Published in [30].

HTCs of about 65 % were measured for the nickel-plated surfaces relative to the copper surface presented in Sec. 4. However, all the tested nickel-plated samples evinced a very stable boiling performance, which was confirmed by the long-term boiling experiments performed additionally. In Fig. 7, a satisfactory agreement is also shown between the measured data and the combination of the pure-fluid correlation of Yagov (9) and the Inoue and Monde mixture correlation (14) which was evaluated using the coefficients recommended by Inoue and Monde [11]. The SEE and MRE between the measured and correlated values are of about 2.2 kW m^{-2} K^{-1} and 12 %, respectively. The combination of the Stephan and Abdelsalam correlation and the Schlünder correlation, which was found to be suitable for the copper surface investigated in Sec. 4, was found not to be applicable for the nickel-plated surfaces.

Own Empirical Correlation for HTC

We developed the empirical correlation

$$\alpha = q^{0.70}\left[1.30\,\mathrm{e}^{-10.6(1-\omega_\mathrm{w})} + 1.18\right] \tag{16}$$

to quickly estimate the HTC for the investigated water–glycerin mixtures, which does not require the thermophysical properties of the boiling mixture. The correlation is valid for the water–glycerin mixtures with ω_w from 1.00

down to 0.60 boiling on smooth nickel surfaces at heat fluxes from 25 up to 650 kW m^{-2}. To use correlation (16), α needs to be in (W m^{-2} K^{-1}), q in (W m^{-2}), and ω_w (−). The values SEE = 1.7 kW m^{-2} and MRE = 11 % were calculated between the measured data and correlation (16). The maximum deviations between the correlated and measured HTCs are mostly comparable with or lower than ±15 %.

Fig. 8 shows the contours of HTC as a function of ω_w and q which was plotted using empirical correlation (16). The contour lines become strongly curved for higher heat fluxes. Smaller HTCs are reached for mixtures with a higher amount of glycerin, relative to the HTCs obtained for pure water. The more straight and almost horizontal contour lines in the right part of Fig. 8 indicate that HTC becomes less dependent on the composition for a lower ω_w.

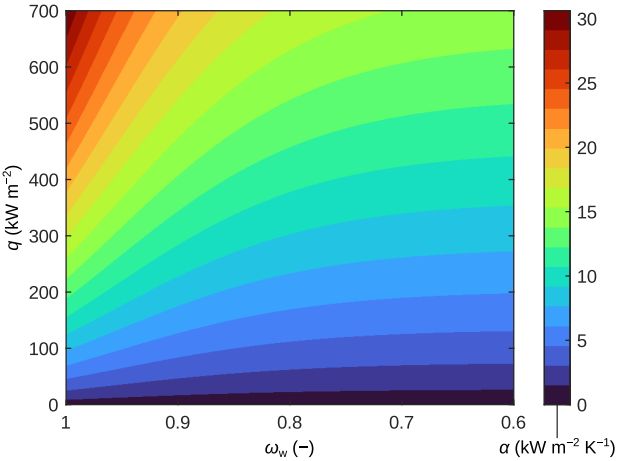

Figure 8: The contour map of the HTCs calculated with empirical correlation (16). Published in [30].

5.4 Results and Discussion for Subcooled Runs

Calculation of HTC during Developed Subcooled Boiling

During the subcooled experiments, a constant value of the temperature of the heating surface was measured throughout each run for all heat flux levels (250, 450, and 650 kW m^{-2}) and samples tested. This is illustrated in Fig. 9 for lower heat fluxes from 200 to 300 kW m^{-2}. The independence of the surface temperature T_s on the subcooling ΔT_{sub} indicates that the developed subcooled boiling regime was reached. In this regime, it is possible to calculate the *total* HTC during subcooled boiling using Eq. (6), where α_b is calculated with

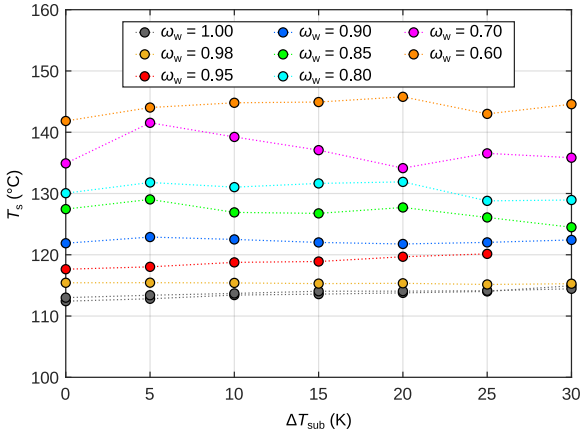

Figure 9: The temperature of the heating surface T_s measured at various levels of subcooling ΔT_{sub}. For clarity, only the data obtained for Sample 1 in the range $200 < q < 300$ kW m^{-2} are shown. Published in [30].

a suitable correlation for saturated boiling. Since the surface temperature T_s remains constant, the *boiling* HTC α_b stays constant as well, and the dependency of α_{tot} on ΔT_{sub} is governed solely by the last fraction in Eq. (6).

Using Own Empirical Correlation

When empirical correlation (16) developed for saturated boiling is employed for the calculation of α_b, the empirical correlation

$$\frac{1}{\alpha_{tot}} = \frac{1}{q^{0.70}\left[1.30\,\mathrm{e}^{-10.6(1-\omega_w)} + 1.18\right]} + \frac{\Delta T_{sub}}{q} \tag{17}$$

is obtained. Correlation (17) produces SEE of about 1.1 kW m^{-2} K^{-1} and MRE below 7 % when compared with the experimental data obtained during subcooled runs. For correlation (17), deviations lower or comparable with ±15 % were obtained for all the measured *total* HTCs as shown in Fig. 10.

Fig. 11 shows the contour map of the *total* HTC as a function of the mass fraction ω_w and subcooling ΔT_{sub}, during subcooled boiling at the heat flux of 300 kW m^{-2}, obtained using empirical correlation (17). The contour lines are more or less straight and diagonal for a higher mass fraction ω_w at all investigated subcoolings ΔT_{sub}. This indicates that for these ranges of ω_w and ΔT_{sub}, neither the subcooling nor the water mass fraction have a dominant effect on the *total* HTC. However, for a lower ω_w, the contour lines are more horizontal which means that the impact of subcooling on the *total* HTC becomes more important

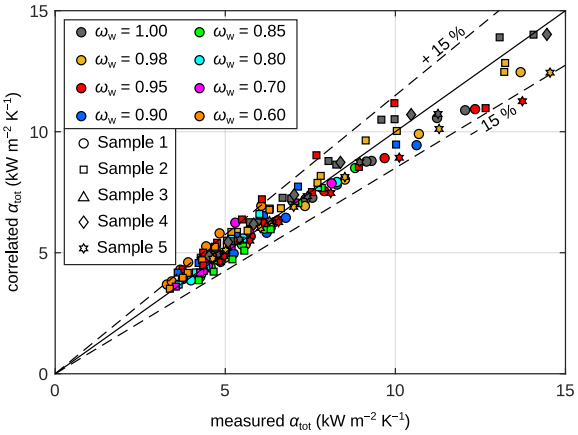

Figure 10: The comparison of the measured *total* HTCs, which were averaged for each of the investigated samples, with the predictions of empirical correlation (17). Published in [30].

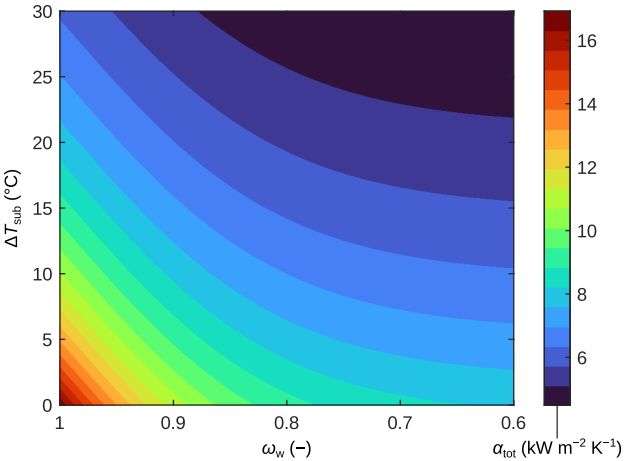

Figure 11: The contour map of the *total* HTC calculated at $q = 300\ \mathrm{kW\,m^{-2}}$ using empirical correlation (17). Published in [30].

relative to the effect of ω_w. Furthermore, the stripes of a constant *total* HTC are closer to each other and more dense in the bottom left corner of the map. This implies that the effect of the subcooling and composition on the *total* HTC is more important for less subcooled mixtures with a lower content of glycerin.

6. Experiments with Thin Titanium Foil

This section presents the measurements of the boiling behavior of water–glycerin mixtures based on infrared (IR) thermometry which enables a detailed analysis of important boiling parameters. A contactless measurement has never been performed before for water–glycerin mixtures. The measurements were conducted for the mixtures with the water mass fractions ω_w from 1.00 down to 0.60. The investigated heat flux was from 1 kW m^{-2} to about 200 kW m^{-2}. The maximum investigated heat flux was lowered for mixtures with a lower ω_w to prevent any thermal damage to the investigated titanium foil. The obtained results presented and discussed in this section were previously published in our article [32].

6.1 Experimental Apparatus

The experiments were performed using the apparatus shown in Fig. 12 designed by the researchers at the Laboratory for Thermal Technology, University of Ljubljana. A single rectangular titanium foil with purity of 99.99 %, thickness δ_{foil} = 25 µm, effective area of 27.6 × 17.7 mm and roughness R_a of about 0.07 µm serves as the heating surface for all the performed experiments. During the measurements, a rectangular window on the bottom side of the foil is monitored with the science-grade IR camera. The foil is heated by the current from a DC power supply. The temperature of the liquid is measured with two TCs immersed in the boiling liquid. An auxiliary heater of a hook-resembling shape is immersed in the liquid to degas the liquid before experiments and to maintain the saturation temperature during the measurements.

6.2 Measurement Uncertainties

The relative propagated uncertainty of the heat flux $u_r(q)$ of about 0.25 % of a measured value was obtained from the propagation of uncertainties related to the quantities used for the calculation of the heat flux [33]. For the conversion of IR images to temperatures, an experimentally measured calibration curve in the range from 80 to 180 °C at steps of 5 °C was employed. During the calibration, the uncertainty of the temperature measurements $u(T)$ = 1 K was determined. Both $u_r(q)$ and $u(T)$ were found to be quite independent of temperature. The thermal sensitivity of the IR camera is less than 20 mK. Such a low value reduces the uncertainty of the temperature differences measured between neighboring pixels to a much lower value than the temperature uncertainty $u(T)$. The maximum uncertainty of HTC $u(\alpha)$, determined from $u_r(q)$ and $u(T)$, was calculated to be of about 1.7 kW m^{-2} K^{-1}. The relative uncertainty of HTC decreases at higher heat fluxes and superheats.

6.3 Results and Discussion

Distributions of Superheat

The distributions of the superheat ΔT_{sat} of the heating surface, calculated with Eq. (2) using the *bubble-point* temperatures T_b measured with the immersed TCs and all the temperatures of the heating surface recorded with the IR camera, were found to be comparable with normal Gaussian distributions, as illustrated in Fig. 13 which shows two examples of histograms obtained at the heat flux $q = 175\ \mathrm{kW\,m^{-2}}$ during boiling of water and the $\omega_w = 0.60$ mixture. Higher superheats characterized by wider distributions were measured for mixtures with a higher glycerin content. The mean value of the superheat ΔT_{sat} and its standard deviation were found to rise slightly and steadily with the increasing concentration of glycerin in the mixture and with increasing heat flux.

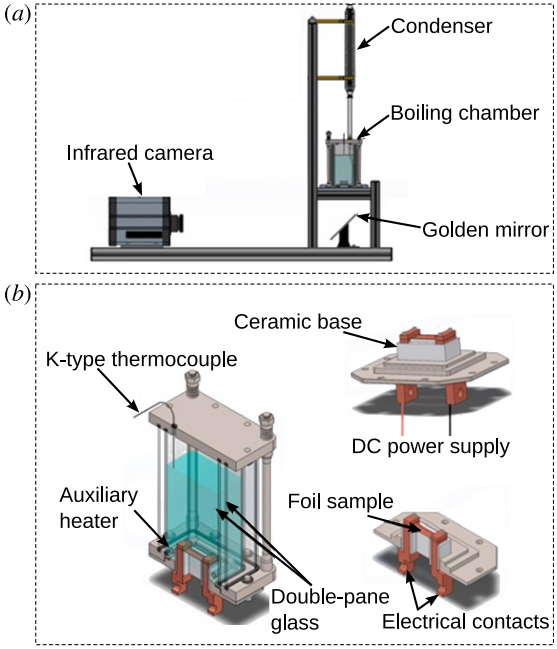

Figure 12: The experimental apparatus for thin foil samples built by the research team at the Laboratory for Thermal Technology: (*a*) side view of the experimental stand, (*b*) detailed view of the boiling chamber and assembly which holds the foil. Adopted from Voglar et al. [33].

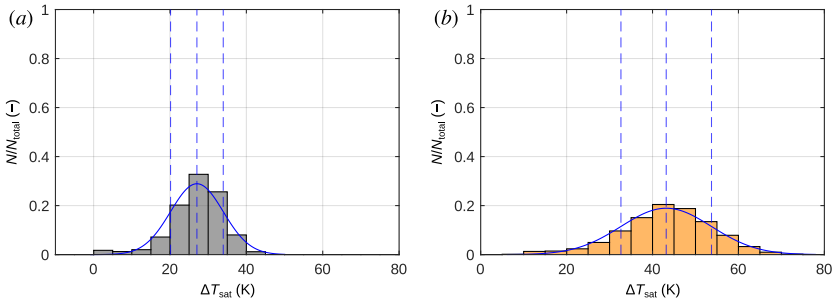

Figure 13: The histograms of the relative probability of the superheats obtained at q = 175 kW m^{-2} for: (*a*) pure water, (*b*) the ω_w = 0.60 mixture. The dashed lines mark the positions of the mean superheat and its standard deviation. The full line is the corresponding normal Gaussian distribution.

Measured HTCs

HTCs were calculated with Eq. (1) by averaging the data recorded with the IR camera. The *bubble-point* temperature T_b was taken as the arithmetic mean of the temperatures measured with both immersed TCs. Fig. 14 shows the dependency of the calculated HTC on the heat flux q and mass fraction ω_w. The

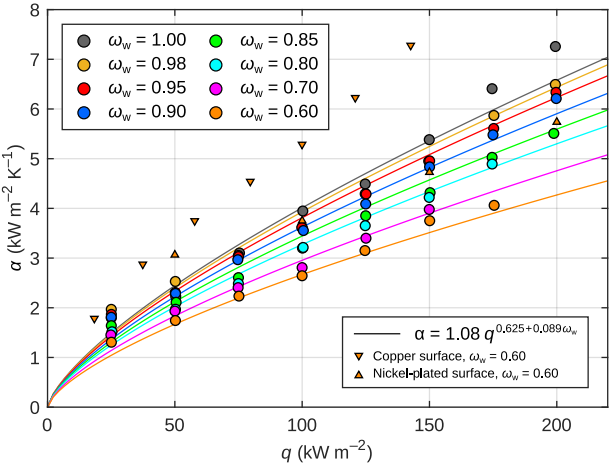

Figure 14: The HTCs obtained from the IR footage after integration in space and time compared with the HTCs measured for the copper and nickel-plated surfaces presented in Sections 4 and 5, respectively. The data are also compared with empirical correlation (18) derived in the following subsection. Published in [32].

measured HTCs are also compared with the data from Sections 4 and 5 obtained for the $\omega_w = 0.60$ mixture. A lower values of HTCs were generally measured for the titanium foil relative to the values measured for the thick copper- and nickel-plated surfaces which might be attributed to the limited number of active nucleation sites observed during boiling on the tested foil or to a small value of the thermal capacity of the foil [34]. Nevertheless, in Fig. 14, the deterioration of HTC for a lower ω_w is clearly visible for higher heat fluxes q, which is consistent with the conclusions presented in Sections 4 and 5.

Own Empirical Correlation for HTC

The measured HTCs might be correlated using the empirical function

$$\alpha = 1.08\, q^{0.625+0.089\omega_w} \tag{18}$$

in the investigated heat flux range from 0 to 200 kW m^{-2} and for water mass fractions from 1.00 down to 0.60. Fig. 14 shows an acceptable agreement between correlation (18) and the measured points. The errors SEE = 0.2 kW m^{-2} K^{-1} and MRE = 6.4 % were calculated between the measured and correlated values. When using correlation (18), the heat flux q has to be in (W m^{-2}), the water mass fraction ω_w (−), and the calculated α is in (W m^{-2} K^{-1}).

Bubble Diameters, Nucleation Frequencies and Bubble Growth Rates

The surface temperatures recorded with the IR camera were analyzed with custom-made scripts which were developed to identify the sudden drops of temperature caused by bubble nucleation. The temporal evolution of temperature fields recorded with the IR camera was used to calculate the nucleation frequency f_n, the maximum footprint diameter D_f (which is assumed to evince similar trends as the bubble departure diameter D_b), and the footprint growth rate $f_n D_f$. The analysis was done for heat fluxes higher than 100 kW m^{-2}.

Tab. 4 show the measured values of the footprint growth rate $f_n D_f$ which are compared with the bubble growth rates $f_n D_b$ predicted by the correlation of Malenkov [35]

$$f_n D_b = \frac{1}{\pi}\left[\frac{D_b\, g\, (\varrho_L - \varrho_G)}{2\,(\varrho_L + \varrho_G)} + \frac{2\,\sigma}{D_b\,(\varrho_L + \varrho_G)}\right]^{1/2} \tag{19}$$

and by the correlation of Peebles and Garber [36]

$$f_n D_b = 0.60\left[\frac{\sigma\, g\, (\varrho_L - \varrho_G)}{\varrho_L^2}\right]^{1/4}. \tag{20}$$

According to Tab. 4, the footprint growth rates measured at higher heat fluxes appears to be comparable with the bubble growth rates predicted with the

Table 4: The measured footprint growth rates $f_n\, D_f$ (mm s^{-1}) compared with the Malenkov correlation and the Peebles and Garber correlation.

		ω_w (−)							
		1.00	0.98	0.95	0.90	0.85	0.80	0.70	0.60
Measured at	q = 100 kW m^{-2}	–	22	18	21	23	28	28	38
	q = 125 kW m^{-2}	19	27	32	31	35	44	44	53
	q = 150 kW m^{-2}	39	35	43	48	53	54	57	55
	q = 175 kW m^{-2}	43	53	58	60	63	66	–	60
	q = 200 kW m^{-2}	59	63	67	74	71	–	–	–
Correlation of	Malenkov (19)	71	70	70	70	70	70	70	69
	Peebles and Garber (20)	92	92	92	92	92	92	91	91

Malenkov correlation. Based on the analysis of the recorded IR footage, the maximum footprint diameter D_f, which oscillated between 3.7 and 5.3 mm, seems to be independent of ω_w, slightly dependent on q and very-well predictable by the often-used correlation of Fritz [37]

$$D_b = 0.0208\, \vartheta_c \sqrt{\frac{\sigma}{g\,(\varrho_L - \varrho_G)}}\,, \tag{21}$$

where the contact angle $\vartheta_c \approx 86°$ was measured for water on titanium foils [38].

On the contrary, the evaluated nucleation frequency f_n was observed to increase significantly with the heat flux and mildly with the concentration of the glycerin in the boiling mixture. The increase of the footprint growth rate $f_n\, D_f$ observed for higher q and ω_w documented in Tab. 4 is thus caused solely by the higher nucleation frequencies.

A series of statistical tests done with the measured data showed that the footprint diameter D_f might be correlated as

$$D_f = 4.54 \times 10^{-2}\, q^{-0.19}\,, \tag{22}$$

and that the nucleation frequency f_n depends on both q and ω_w and might be approximated with the function

$$f_n = 8.88 \times 10^{-9}\, \frac{q^{1.73}}{\omega_w}\,. \tag{23}$$

Combining Eq. (22) and (23), the footprint growth rate (i.e., the growth of the zones affected by bubble nucleation) might be estimated with the correlation

$$f_n\, D_f = 4.03 \times 10^{-10}\, \frac{q^{1.54}}{\omega_w}\,. \tag{24}$$

Correlations (22) to (24) are valid for the ranges of water mass fraction $0.60 \leq \omega_w \leq 1.00$ and heat flux $100 \leq q \leq 200$ kW m^{-2}. To use correlations (22)

to (24), q needs to be in (W m^{-2}), ω_w is dimensionless, D_f is given in (m), f_n is in (s^{-1}) and $f_n D_f$ in (m s^{-1}).

Thermal Energy Consumed by Bubbles

Since the footprint diameter D_f (which represents the bubble departure diameter) was found to be a weak function of q independent of the concentration of the boiling mixture, and since the nucleation frequency f_n seems to increase with a decrease of ω_w, the deterioration of HTC observed for a low ω_w cannot be related to the trends of the investigated parameters. A possible cause of the HTC deterioration might be a lower intensity of heat transfer, even despite the increased nucleation frequencies and bubble growth rates. This was analyzed by evaluation of the average thermal energy Q_b consumed during individual nucleation cycles which might be defined as

$$Q_b = \int_{t_g} \left(\iint_{S_{affected}} q \, dS \right) dt \, , \tag{25}$$

where the integrals in Eq. (25) were approximated by sums over the pixels of the IR footage, which were affected by bubble nucleation.

The analysis of the resulting values of Q_b did not result in a clear trend of the thermal energy Q_b with respect to the heat flux q and water mass fraction of the mixture ω_w. A series of statistical tests indicated that Q_b is likely a constant independent of q and ω_w investigated. A mean value of Q_b about 46 mJ and a standard deviation of 8 mJ were evaluated from the analysis of the IR data.

Suggested Explanation of the Measured HTC Deterioration

The measured values and trends of the evaluated parameters suggest that the the measured decrease of HTC with ω_w is probably not directly related to the transport of latent heat by nucleating bubbles. Therefore, the measured deterioration of HTC is likely caused by reduced heat transfer into the liquid phase as a consequence of lower intensity of enhanced convection, transient conduction, and natural convection. The deterioration of heat transfer might be explained to be caused by retardation of convective mechanisms due to the increased viscosity, increased density, or decreased specific heat capacity of the mixtures with a higher content of glycerin.

7. Recapitulation of Experiments and Outputs

7.1 Boiling of Water–Glycerin Mixtures on the Copper Surface

Performed Experiments

- The commonly-used steady-state method of measurement and the own dynamic measurement method were applied.
- A single copper block with a smooth planar heating surface (R_a of 0.4 µm) was investigated.
- The water mass fractions $0.40 \leq \omega_w \leq 1.00$ and heat fluxes $25 \leq q \leq 270\ \mathrm{kW\,m^{-2}}$ were studied.
- In total, 9 experimental runs were performed and 109 data points obtained.

Outputs

- The empirical correlation for HTC (SEE = $0.5\ \mathrm{kW\,m^{-2}\,K^{-1}}$, MRE = 6 %)

$$\alpha = 0.59\, q^{0.714+0.130\omega_w}\ .$$

- The proposed and verified dynamic method.

Published in

- Vajc V., Šulc R., Dostál M., Pool Boiling Heat Transfer Coefficients in Mixtures of Water and Glycerin, *Processes*, vol. 9, no. 5, article no. 830, May 2021, pp. 1–19. doi:10.3390/pr9050830.

7.2 Boiling of Water–Glycerin Mixtures on the Nickel-Plated Surfaces

Performed Experiments

- HTCs during saturated and subcooled boiling were measured.
- Five nickel-plated surfaces with a smooth planar heating surface (R_a about 0.4 µm) were investigated.
- The water mass fractions $0.60 \leq \omega_w \leq 1.00$ and heat fluxes $0 \leq q \leq 650\ \mathrm{kW\,m^{-2}}$ were studied.
- Subcooled experiments were done for $q = 250$, 450, and $650\ \mathrm{kW\,m^{-2}}$ at the subcooling $0 \leq \Delta T_{sub} \leq 30$ K.
- Long-term measurements of the performance stability were conducted.
- In total, 110 saturated and 82 subcooled runs were performed.

Outputs

- The empirical correlation for the HTC during saturated boiling (SEE = $1.7\ \mathrm{kW\,m^{-2}\,K^{-1}}$, MRE = 11 %)

$$\alpha = q^{0.70}\left[1.30\,\mathrm{e}^{-10.6(1-\omega_w)} + 1.18\right].$$

- The empirical correlation for the *total* HTC during subcooled boiling (MRE = 7 %, SEE = $1.1\ \mathrm{kW\,m^{-2}\,K^{-1}}$)

$$\frac{1}{\alpha_{tot}} = \frac{1}{q^{0.70}\left[1.30\,\mathrm{e}^{-10.6(1-\omega_w)} + 1.18\right]} + \frac{\Delta T_{sub}}{q}\ .$$

Published in

- Vajc V., Može M., Hadžić A., Zupančič M., Golobič I., Saturated and Subcooled Pool Boiling Heat Transfer in Mixtures of Water and Glycerin, *Experimental Heat Transfer*, Jan. 2022. doi:10.1080/08916152.2022.2027574.

7.3 Boiling of Water–Glycerin Mixtures on the Titanium Foil

Performed Experiments

- Infrared thermometry was applied to measure the temperature distribution of the heating surface in space and time.
- A single titanium foil ($R_a = 0.07$ µm, $\delta_{foil} = 25$ µm) was investigated.
- The water mass fractions $0.60 \leq \omega_w \leq 1.00$ and heat fluxes $0 \leq q \leq 200$ kW m^{-2} were studied.
- In total, 155 IR videos were captured. Two runs were performed for each of the eight investigated concentrations. Each run contained from 8 to 11 measurements at discrete heat flux levels.

Outputs

- The empirical correlation for the HTC during saturated boiling (SEE = 1.7 kW m^{-2} K^{-1}, MRE = 11 %)
$$\alpha = 1.08\, q^{0.625+0.089\omega_w} .$$
- The empirical correlation for the measured diameter of the temperature footprint of bubbles
$$D_f = 4.54 \times 10^{-2}\, q^{-0.19} .$$
- The empirical correlation for the measured nucleation frequency
$$f_n = 8.88 \times 10^{-9}\, \frac{q^{1.73}}{\omega_w} .$$
- The empirical correlation for the measured growth rate of temperature footprints
$$f_n = 4.03 \times 10^{-10}\, \frac{q^{1.54}}{\omega_w} .$$

Published in

- Vajc V., Može M., Zupančič M., Šulc R., Golobič I., IR Measurements of Heat Transfer Coefficients and Nucleation Parameters during Saturated Nucleate Boiling of Water–Glycerin Mixtures, *Case Studies in Thermal Engineering*, vol. 32, article 101917, Apr. 2022, pp. 1–13. doi:10.1016/j.csite.2022.101917.

8. Conclusions

The following conclusions based on the experimental results presented in the experimental part might be drawn for the investigated water–glycerin mixtures:

- HTC deteriorates with an increasing amount of the less volatile component (glycerin) in water–glycerin mixtures. This was observed for all of the investigated surfaces (copper, nickel-plated and titanium), heat fluxes, and concentrations of the boiling mixture.
- The *mixture effects* were found to affect the HTC during boiling of water–glycerin mixtures on all surfaces and compositions investigated.
- HTC enhancement was not detected for any of the concentrations and heating surfaces investigated.
- The investigated nickel-plated and titanium surfaces maintained a stable boiling performance during multiple repeated runs. The stability of nickel-plated samples was confirmed by long-term boiling experiments.
- Bubble departure diameters were found to be weakly dependent on the heat flux, independent of the concentration, and well predictable by the often-used correlation of Fritz.
- The nucleation frequencies increased significantly with the heat flux and gradually with the concentration of glycerin in the boiling mixture. The measured increase of the bubble growth rate was caused solely by the increase of the nucleation frequency.
- The thermal energy transferred into nucleating bubbles of about 46 ± 8 mJ was found to be independent of the heat flux and concentration.
- Trends of the investigated boiling parameters measured for the titanium heating surface indicate that heat transfer to the liquid phase by convective mechanisms is more important than the mechanisms related to the transport of latent heat.
- The subcooled boiling experiments proved that when the developed regime of subcooled boiling is achieved, the correlations suitable for saturated boiling might be employed to predict the HTCs during subcooled boiling.
- The effects of the subcooling and composition on the *total* HTC were observed to be more important for the less subcooled mixtures with lower glycerin content.
- The HTCs measured for the investigated titanium foil were of about 45 % and 70 % relative to those measured for the copper and nickel-plated surfaces, respectively. The HTCs measured for the nickel-plated surfaces reached approximately 65 % relative to those measured for the copper surface.

The data and information presented in and related to this thesis were previously published in the author's works [24,27,28,30,32,39].

References

[1] El-Genk M.S., Parker J.L., Nucleate Boiling of FC-72 and HFE-7100 on Porous Graphite at Different Orientations and Liquid Subcooling, *Energy Conversion and Management*, vol. 49, no. 4, Apr. 2008, pp. 733–750. doi:10.1016/j.enconman.2007.07.028.

[2] Stephan K., *Heat Transfer in Condensation and Boiling*. Berlin, Germany: Springer Berlin Heidelberg, 1992. doi:10.1007/978-3-642-52457-8.

[3] Stephan K., Abdelsalam M., Heat-Transfer Correlations for Natural Convection Boiling, *International Journal of Heat and Mass Transfer*, vol. 23, no. 1, Jan. 1980, pp. 73–87. doi:10.1016/0017-9310(80)90140-4.

[4] Yagov V.V., Generic features and puzzles of nucleate boiling, *International Journal of Heat and Mass Transfer*, vol. 52, no. 21, Oct. 2009, pp. 5241–5249. doi:10.1016/j.ijheatmasstransfer.2009.03.071.

[5] Fujita Y., Tsutsui M., Heat Transfer in Nucleate Pool Boiling of Binary Mixtures, *International Journal of Heat and Mass Transfer*, vol. 37, Mar. 1994, pp. 291–302. doi:10.1016/0017-9310(94)90030-2.

[6] Dang C., Jia L., Peng Q., Huang Q., Zhang X., Experimental and Analytical Study on Nucleate Pool Boiling Heat Transfer of R134a/R245fa Zeotropic Mixtures, *International Journal of Heat and Mass Transfer*, vol. 119, Apr. 2018, pp. 508–522. doi:10.1016/j.ijheatmasstransfer.2017.11.143.

[7] Park K.J., Jung D., Nucleate Boiling Heat Transfer Coefficients of Mixtures Containing Propane, Isobutane and HFC134a, *Journal of Mechanical Science and Technology*, vol. 20, no. 3, 2006, pp. 399–408. doi:10.1007/BF02917523.

[8] Fujita Y., Tsutsui M., Nucleate Boiling of Two and Three-Component Mixtures, *International Journal of Heat and Mass Transfer*, vol. 47, no. 21, Oct. 2004, pp. 4637–4648. doi:10.1016/j.ijheatmasstransfer.2003.09.039.

[9] Schlünder E.U., Heat Transfer in Nucleate Boiling of Mixtures, *International Chemical Engineering*, vol. 23, no. 4, 1983, pp. 589–599.

[10] Thome J.R., Shakir S., A New Correlation for Nucleate Pool Boiling of Aqueous Mixtures, in *Proceedings of the Eighth International Heat Transfer Conference*, vol. 18 (9), (USA), INIS, 1987.

[11] Inoue T., Monde M., Prediction of Pool Boiling Heat Transfer Coefficient in Ammonia/Water Mixtures, *Heat Transfer—Asian Research*, vol. 38, no. 2, 2009, pp. 65–72. doi:10.1002/htj.20234.

[12] Inoue T., Kawae N., Monde M., Characteristics of Heat Transfer Coefficient During Nucleate Pool Boiling of Binary Mixtures, *Heat and Mass Transfer*, vol. 33, no. 4, Feb. 1998, pp. 337–344. doi:10.1007/s002310050199.

[13] Wiley-VCH, *Ullmann's Encyclopedia of Industrial Chemistry*. 40 Volume Set, Wiley-VCH Verlag GmbH & Co. KGaA, ISBN 978-3-527-32943-4, Aug. 2011.

[14] OECD, OECD-FAO Agricultural Outlook (Edition 2021), Tech. Rep., Organisation for Economic Co-operation and Development, Paris, 2021. Available at: https://www.oecd-ilibrary.org/agriculture-and-food/data/oecd-agriculture-statistics/oecd-fao-agricultural-outlook-edition-2021_4bde2d83-en.

[15] The Soap and Detergent Association, *Glycerine: An Overview*. New York, NY, USA: Glycerine & Oleochemical Division, 1990.

[16] Mokbel I., Sawaya T., Zanota M.L., Naccoul R.A., Jose J., de Bellefon C., Vapor–Liquid Equilibria of Glycerol, 1,3-Propanediol, Glycerol + Water, and Glycerol + 1,3-Propanediol, *Journal of Chemical & Engineering Data*, vol. 57, no. 2, Feb. 2012, pp. 284–289. doi:10.1021/je200766t.

[17] Tolubinsky V.I., Ostrovsky Y.N., Kriveshko A.A., Heat Transfer to Boiling Water-Glycerine Mixtures, *Heat Transfer–Soviet Research*, vol. 2, no. 1, 1970, pp. 22–24.

[18] Sternling C.V., Tichacek L.J., Heat Transfer Coefficients for Boiling Mixtures: Experimental Data for Binary Mixtures of Large Relative Volatility, *Chemical Engineering Science*, vol. 16, no. 3, Dec. 1961, pp. 297–337. doi:10.1016/0009-2509(61)80040-7.

[19] Sarafraz M.M., Peyghambarzadeh S.M., Influence of Thermodynamic Models on the Prediction of Pool Boiling Heat Transfer Coefficient of Dilute Binary Mixtures, *International Communications in Heat and Mass Transfer*, vol. 39, no. 8, Oct. 2012, pp. 1303–1310. doi:10.1016/j.icheatmasstransfer.2012.06.020.

[20] Alavi Fazel S.A., Sarafraz M., Arabi Shamsabadi A., Peyghambarzadeh S.M., Pool Boiling Heat Transfer in Diluted Water/Glycerol Binary Solutions, *Heat Transfer Engineering*, vol. 34, no. 10, Aug. 2013, pp. 828–837. doi:10.1080/01457632.2012.746157.

[21] Kuo W.C., *Thermal Decomposition Of Aqueous Glycerine Mixtures, Ethyl Acetate, Diethyl Carbonate, And Ethanol At High Temperatures In A Film Boiling Reactor*. PhD thesis, Cornell University, Ithaka, NY, USA, Aug. 2014. Available at: https://ecommons.cornell.edu/handle/1813/38943.

[22] McNeil D.A., Burnside B.M., Elsaye E.A., Salem S.M., Baker S., Shell-Side Boiling of a Glycerol-Water Mixture at Low Sub-Atmospheric Pressures, *Applied Thermal Engineering*, vol. 115, Mar. 2017, pp. 1438–1450. doi:10.1016/j.applthermaleng.2016.11.169.

[23] Yang B., Sarafraz M.M., Arjomandi M., Marangoni Effect on the Thermal Performance of Glycerol/Water Mixture in Microchannel, *Applied Thermal Engineering*, vol. 161, Oct. 2019, p. 114142. doi:10.1016/j.applthermaleng.2019.114142.

[24] Vajc V., Šulc R., Dostál M., Pool Boiling Heat Transfer Coefficients in Mixtures of Water and Glycerin, *Processes*, vol. 9, no. 5, article no. 830, May 2021, pp. 1–19. doi:10.3390/pr9050830.

[25] Može M., Zupančič M., Hočevar M., Golobič I., Gregorčič P., Surface Chemistry and Morphology Transition Induced by Critical Heat Flux Incipience on Laser-Textured Copper Surfaces, *Applied Surface Science*, vol. 490, Oct. 2019, pp. 220–230. doi:10.1016/j.apsusc.2019.06.068.

[26] Može M., Zupančič M., Golobič I., Pattern Geometry Optimization on Superbiphilic Aluminum Surfaces for Enhanced Pool Boiling Heat Transfer, *International Journal of Heat and Mass Transfer*, vol. 161, Nov. 2020, p. 120265. doi:10.1016/j.ijheatmasstransfer.2020.120265.

[27] Može M., Vajc V., Zupančič M., Šulc R., Golobič I., Pool Boiling Performance of Water and Self-Rewetting Fluids on Hybrid Functionalized Aluminum Surfaces, *Processes*, vol. 9, no. 6, June 2021, pp. 1–27. doi:10.3390/pr9061058.

[28] Može M., Vajc V., Zupančič M., Golobič I., Hydrophilic and Hydrophobic Nanostructured Copper Surfaces for Efficient Pool Boiling Heat Transfer with Water, Water/Butanol Mixtures and Novec 649, *Nanomaterials*, vol. 11, no. 12, Dec. 2021, pp. 1–24. doi:10.3390/nano11123216.

[29] Može M., Effect of Boiling-Induced Aging on Pool Boiling Heat Transfer Performance of Untreated and Laser-Textured Copper Surfaces, *Applied Thermal Engineering*, vol. 181, Nov. 2020, p. 116025. doi:10.1016/j.applthermaleng.2020.116025.

[30] Vajc V., Može M., Hadžić A., Šulc R., Golobič I., Saturated and Subcooled Pool Boiling Heat Transfer in Mixtures of Water and Glycerin, *Experimental Heat Transfer*, vol. 0, no. 0, Jan. 2022, pp. 1–29. doi:10.1080/08916152.2022.2027574.

[31] Može M., Zupančič M., Golobič I., Investigation of the Scatter in Reported Pool Boiling CHF Measurements Including Analysis of Heat Flux and Measurement Uncertainty Evaluation Methodology, *Applied Thermal Engineering*, vol. 169, Mar. 2020, p. 114938. doi:10.1016/j.applthermaleng.2020.114938.

[32] Vajc V., Može M., Zupančič M., Šulc R., Golobič I., IR Measurements of Heat Transfer Coefficients and Nucleation Parameters During Saturated Nucleate Boiling of Water–Glycerin Mixtures, *Case Studies in Thermal Engineering*, vol. 32, article no. 101917, Apr. 2022, pp. 1–13. doi:10.1016/j.csite.2022.101917.

[33] Voglar J., Zupančič M., Peperko A., Birbarah P., Miljkovic N., Golobič I., Analysis of Heater-Wall Temperature Distributions During the Saturated Pool Boiling of Water, *Experimental Thermal and Fluid Science*, vol. 102, Apr. 2019, pp. 205–214. doi:10.1016/j.expthermflusci.2018.11.012.

[34] Zupančič M., Gregorčič P., Bucci M., Wang C., Matana Aguiar G., Bucci M., The Wall Heat Flux Partitioning During the Pool Boiling of Water on Thin Metallic Foils, *Applied Thermal Engineering*, vol. 200, Jan. 2022, p. 117638. doi:10.1016/j.applthermaleng.2021.117638.

[35] Malenkov I., The Frequency of Vapor-Bubble Separation as a Function of Bubble Size, *Fluid Mechanics-Soviet Research*, vol. 1, no. 143, 1972, pp. 36–42.

[36] Peebles F.N., Garber H.J., Studies on the Motion of Gas Bubbles in Liquid, *Chemical Engineering Progress*, vol. 49, no. 2, 1953, pp. 88–97. Available at: https://ci.nii.ac.jp/naid/10006284049/.

[37] Fritz W., Maximum Volume of Vapor Bubbles, *Physikalische Zeitschrift*, vol. 36, no. 11, 1935, pp. 379–384.

[38] Petkovsek J., Heng Y., Zupančič M., Gjerkes H., Cimerman F., Golobič I., IR Thermographic Investigation of Nucleate Pool Boiling at High Heat Flux, *International Journal of Refrigeration*, vol. 61, Jan. 2016, pp. 127–139. doi:10.1016/j.ijrefrig.2015.10.018.

[39] Vajc V., *Pool Boiling (master's thesis)*. Prague, Czech Republic: Czech Technical University in Prague, 2017. Available at: https://dspace.cvut.cz/handle/10467/73374.

Author's Publications

Articles in Impacted Journals

- Vajc V., Može M., Zupančič M., Šulc R., Golobič I., IR Measurements of Heat Transfer Coefficients and Nucleation Parameters during Saturated Nucleate Boiling of Water–Glycerin Mixtures, *Case Studies in Thermal Engineering*, vol. 32, Apr. 2022. doi:10.1016/j.csite.2022.101917.
- Vajc V., Može M., Hadžić A., Zupančič M., Golobič I., Saturated and Subcooled Pool Boiling Heat Transfer in Mixtures of Water and Glycerin, *Experimental Heat Transfer*, Jan. 2022, pp. 1–29. doi:10.1080/08916152.2022.2027574.
- Vajc V., Šulc R., Dostál M., Pool Boiling Heat Transfer Coefficients in Mixtures of Water and Glycerin, *Processes*, vol. 9, no. 5, article no. 830, May 2021, pp. 1–19. doi:10.3390/pr9050830.
- Može M., Vajc V., Zupančič M., Golobič I., Hydrophilic and Hydrophobic Nanostructured Copper Surfaces for Efficient Pool Boiling Heat Transfer with Water, Water/Butanol Mixtures and Novec 649, *Nanomaterials*, vol. 11, no. 12, article no. 3216, Dec. 2021, pp. 1–24. doi:10.3390/nano11123216.
- Može M., Vajc V., Zupančič M., Šulc R., Golobič I., Pool Boiling Performance of Water and Self-Rewetting Fluids on Hybrid Functionalized Aluminum Surfaces, *Processes*, vol. 9, no. 6, article no. 1058, June 2021, pp. 1–27. doi:10.3390/pr9061058.

Indexed Conference Contributions

- Vajc V., Dostál M., First Testing Experiments with Measurement of Pool Boiling Heat Transfer Coefficient on a New Apparatus, in *Proceedings of Experimental Fluid Mechanics 2018 Conference (EFM 2018)*, Les Ulis Cedex, France: EDP Sciences, EPJ Web of Conferences. vol. 213., 2019, pp. 1–5, ISSN 2100-014X. Available at: https://www.epj-conferences.org/articles/epjconf/pdf/2019/18/epjconf_efm18_02090.pdf.

Other Conference Contributions

- Vajc V., Dostál M., Fixation of Thermocouples and Insulation for Heated Block, in *Advances in Heat Transfer and Thermal Engineering, Proceedings of 16th UK Heat Transfer Conference (UKHTC2019)*, Springer Nature Singapore Pte Ltd., vol. 1, 2021. pp. 71–77. ISBN 978-981-334-764-9, doi:10.1007/978-981-33-4765-6_13.
- Vajc V., Dostál M., How Does Uncertainty of Thermal Conductivity Impact Measurements of Pool Boiling Heat Transfer Coefficient?, in: *Proceedings of the 8th International Conference on Chemical Technology*. Prague, Czech Republic: Czech Society of Industrial Chemistry, 2021, pp. 316–320.

ISBN 978-80-88307-08-2. Available at: https://www.icct.cz/cs/Amca-ICCT/media/content/2021/proceedings/ICCT2021-Proceedings.pdf.

- Vajc V., Dostál M., How to Improve a Temperature Distribution inside a Heated Block in a Typical Pool-Boiling Apparatus, in *Proceedings of the 14th International Conference on Heat Transfer, Fluid Mechanics and Thermodynamics (HEFAT2019)*. Caps Town, South Africa: HEFAT, 2019, pp. 808–813. ISBN 978-1-77592-191-2. Available at: https://bit.ly/3oZXixp.
- Vajc V., Dostál M., Pool Boiling, in *Book of Abstracts, Full Papers of 6th International Conference on Chemical Technology*, Prague, Czech Republic: Czech Society of Industrial Chemistry, 2018. Available at: https://dev8-admin.morbo.puxdesign.cz/Amca-ICCT/media/content/2018/ICCT-2018-Proceedings.pdf.
- Vajc V., Multicomponent Boiling and Tube-Bundle Boiling with Focus on Heat Transfer, unpublished lecture from the conference *Energie z Biomasy*, Brno University of Technology, Faculty of Mechanical Engineering, Energy Institute, Sep. 2018.
- Vajc V., Heat Transfer in Pool Boiling, in *Proceedings of CHISA 2017 Conference*, Prague, Czech Republic: Czech Society of Chemical Engineering, Oct. 2017, pp. 157.

Functional Sample

- Vajc V., Dostál M., Laboratory Apparatus for Measurement of Heat Transfer Coefficient during Pool Boiling, 2020, identification label U12118-FVZ-2020-1, identification no. VV-2020-Var-01.

Master's Thesis

- Vajc V., *Pool boiling (master's thesis).* Prague, Czech Republic: Czech Technical University in Prague, 2017. Available at: https://dspace.cvut.cz/handle/10467/73374.